The genesis of convective clouds

Leif Denby[1] Steven Boeing[1] Doug Parker[1] Michael Whitall[2]
[1]University of Leeds [2]MetOffice

UNIVERSITY OF LEEDS

Aim

Characterise coherent boundary-layer structures which cause the formation of moist-convective updrafts (i.e. convective clouds).

- What are the spatial scales of boundary-layer updrafts? Horizontal aspect ratio? Spatial distribution (spatial separation)?
- What influences these characteristics? I.e. how do these characteristics change with the boundary layer state?
- How do specific phenomena related to moist convection (shallow/deep convection, squall lines, coldpools, etc) affect these?
- Does the topology of these coherent structures influence their dynamical behaviour? Can the topology be used as a means of classification (instead of isosurfaces)?

So as to

- Identify which physical variables are most important to represent convective trigger, which variables carry memory.
- Provide convective scheme with joint distributions (e.g. $P(q_t, \theta_l, w)$) of cloud-base conditions and canonical shape of coherent structures to aid modelling

Simulations overview

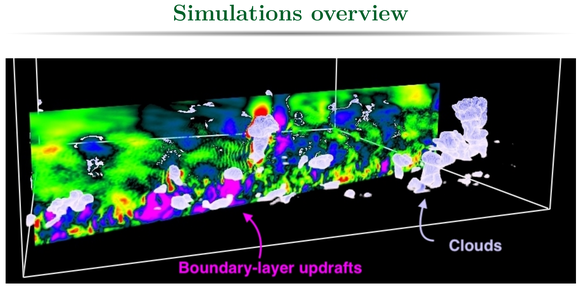

Figure 1: Radiative-Convective Equilibrium precipitating marine shallow cumulus based on RICO measuring campaign. Using UCLA-LES (Stevens et al., 2005). Individual clouds identified with cloud-tracking algorithm (Heus & Seifert, 2013)

Multiple ($O(10^4)$) interacting clouds triggered through surface-fluxes and large-scale forcing in large domain ($O(10)km^2$) LES ($\Delta x = 25m$). Original RICO case (VanZanten et al., 2011) and RICO-like with fixed surface fluxes and with/without ambient windshear.

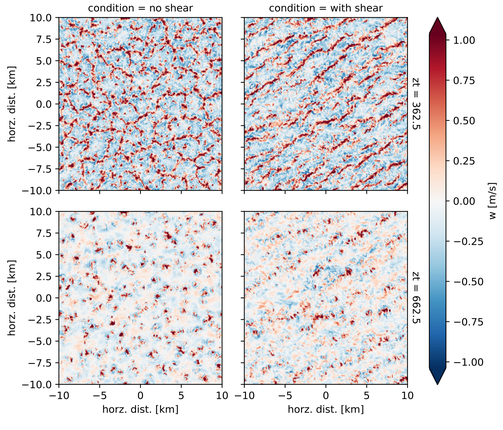

Figure 2: Horizontal cross-sections of vertical velocity through the boundary-layer middle ($z \approx 350$m, top) and at cloud-base height ($z \approx 650$m, bottom) for simulations with shear (right) and without (left). The presence of ambient shear breaks the geometry of convective cells and create elongated coherent boundary structures.

Analysis methods

Cumulant analysis

In Tobias & Marston (2016) cumulants (higher-order generalisation of covariance) were applied to identify the principle length-scales of coherent structures in 3D Couvette flow. For example computing the second cumulant for velocity at two different heights (z_1 and z_2) is given by

$$c_{uu}(\xi, \mu, z_1, z_2) = \frac{1}{L_x L_y} \int_0^{L_x} \int_0^{L_y} u'(x, y, z_1) u'(x + \xi, y + \nu, z_2) dx dy.$$

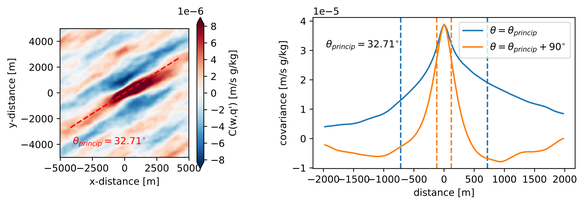

Figure 3: 2nd cumulant (left) for moisture q and vertical velocity w in the middle of the boundary layer ($z = 300$m) as well as samplings (right) of the cumulant along the identified *principle axis* and orthogonal to this in simulation with ambient shear. The cumulant effectively displays the coherence length of the vertical moisture flux, making it possible to quantify the elongation of coherent structures by ambient shear by calculating an integral length-scale in the two directions (vertical lines).

Topological measures

Zhdankin et al. (2014) studied energy dissipation in magnetohydrodynamic turbulence through topological measures (Minkowski functionals) of structures identified by isosurfaces of current density. Found that majority of transport done by long thin filaments. Aim to use this method to classify through their topology the coherent structures in the convective boundary layer which dominate transport of moisture and heat to trigger convective clouds.

In 3D the Minkowski functionals are

$$V_0 = V = \int dV$$
$$V_1 = \frac{A}{6} = \frac{1}{6} \int dS$$
$$V_2 = \frac{H}{3\pi} = -\frac{1}{6\pi} \int dS \nabla \cdot \hat{\mathbf{n}} = \frac{1}{6\pi} \int (\kappa_1 + \kappa_2) dS$$
$$V_3 = \frac{1}{4\pi} \int (\kappa_1 \kappa_2) dS$$

From these a characteristic *length* (L_m), *width* (W_m) and *thickness* (T_m) can be calculated as

$$L_m = \frac{3V_2}{4V_3}, W_m = \frac{2V_1}{\pi V_2}, T_m = \frac{V_0}{2V_1},$$

where the normalization is so that all measures correspond to the radius when applied to a sphere.

These may be further reduced as *filamentarity* (F_m) and *planarity* (P_m):

$$F_m = \frac{L_m - W_m}{L_m + W_m}, P_m = \frac{W_m - T_m}{W_m + T_m},$$

which measure whether objects are more pencil (high filamentarity) or pancake-like (high planarity).

Coherent structures in the boundary layer are identified using the method pioneered by Couvreux et al. (2010) in which the concentration a surface released radioactive (decaying) passive tracer (ϕ) is normalized by its variance in the domain-wide horizontal cross-section at a given height $\sigma_\phi(z)$. This method was verified by comparing with the at cloud-base values of thermodynamic properties of newly formed clouds (see Figure 4)

Results - bulk properties

For all results cloud-base was at $z_{base} \approx 650m$.

Identification of cloud-triggering structures

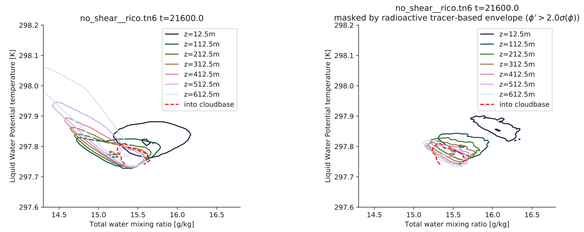

Figure 4: Joint distributions of water vapour and potential temperature in horizontal cross-sections at increasing heights in the full boundary layer together (left) and only regions where the radioactive scalar $\mu > 2\sigma_\phi$. For comparison the distributions for air entering through cloudbase for newly formed clouds ($t_a ge < 3$min) are included, indicating that the radioactive tracer identifies air with cloud-triggering properties.

Charactistic length-scales of vertical transport

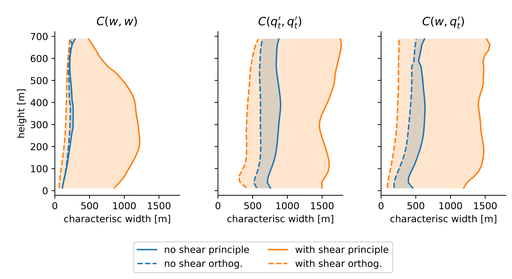

Figure 5: Vertical profiles of cumulant derived length-scales for vertical velocity (left), water vapour (center) and covariance (right). The minimum and maximum length-scales (along the principle and perpendicular directions respectively) are shown for each variable for both simulations with (orange) and without (blue) shear. All cumulants indicate that shear causes elongation (see direction of elongation in Figure 6 below), and effects the water vapour field more strongly than vertical velocity. In addition vertical velocity suggests structures which are widest in the bulk of the boundary layer, whereas moisture flux is near constant above $z \approx 100$m

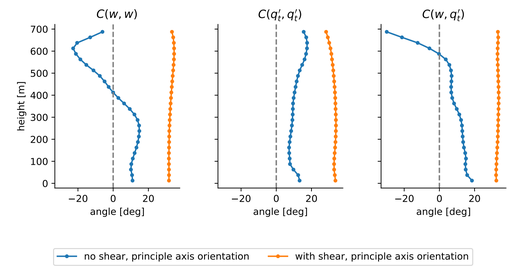

Figure 6: Vertical profiles of the angle of elongation derived from the cumulants of vertical velocity (left), water vapour (center) and their covariance (right). The direction of elongation in presence of ambient shear is near constant with height for all three cumulants, only for for water vapour does the direction veer off near cloud-base. The simulations without shear show an interesting change in orientation with height, however as seen in Figure 5 the actual aspect ratio of elongation is near unity so the angle is of little relevance in the non-sheared case

Results - individual objects

Shape of individual coherent structures

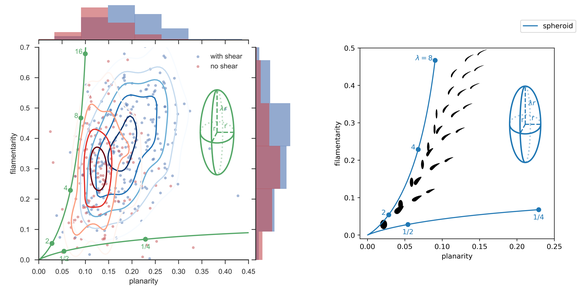

Figure 7: Joint distribution of filamentarity and planarity (left) for the largest objects cumulatively contributing 90% of the total moisture fluxes in the cases with (in blue) and without (in red) shear, together with same computed for synthetic shapes plotted using outline of shapes (right). Shear causes elongation and widening of the coherent structures. The points in the left figure represent individual objects and the contours were created from a local kernel density estimate connecting individual points by a Gaussian kernel.

Object tilt and orientation

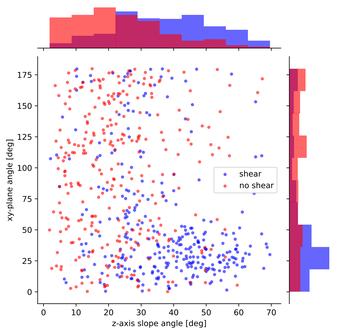

Figure 8: Tilt vs xy-plane orientation for individual objects (with effective radius $r > 100$m) under sheared (blue) and un-sheared (red) conditions. The presences of ambient shear is seen to to tilt individual objects by $\approx 20 - 40°$ and cause the objects to orient in the direction of shear

Further work

- Study thermodynamic properties of cloud triggering coherent structures.
- Develop predictive model for distribution of thermal size as well as physical properties at cloud base

References

Couvreux, F., Hourdin, F., & Rio, C. 2010, Boundary-Layer Meteorology, 134, 441

Heus, T. & Seifert, a. 2013, Geoscientific Model Development, 6, 1261

Stevens, B., Moeng, C.-H., Ackerman, A. S., et al. 2005, Monthly Weather Review, 133, 1443

Tobias, S. & Marston, B. 2016, 412

VanZanten, M. C., Stevens, B., Nuijens, L., et al. 2011, Journal of Advances in Modeling Earth Systems, 3

Zhdankin, V., Boldyrev, S., Perez, J. C., & Tobias, S. M. 2014, 1